Quadratically Constrained Quadratic Programs for Mismatched Filter Optimization with Radar Applications

O. Rabaste, L. Savy

Quadratically Constrained Quadratic Programs for Mismatched Filter Optimization with Radar Applications

Olivier Rabaste, Laurent Savy

01

e Guinebretiere

***Abstract*—In this article, we consider the problem of optimal filter computation. The contribution of this paper is three-fold. First we propose a new method for finding the mismatched filter that minimizes the Peak-to-Sidelobe Ratio. While existing solutions solve this problem only approximately, the proposed method, based on a reformulation of the optimization problem as a convex quadratically constrained quadratic program (QCQP), insures that any found solution is a global solution of the problem. This formulation also permits to insert additional constraints, for instance a constraint on the loss in processing gain of the optimal filter. We study in this context the robustness of the proposed filter to phase errors. Second we show that the proposed QCQP can easily be adapted to deal with doppler shifts and provide results for specific applications. Third we investigate the possibility to use mismatched filters to reduce the high sidelobe level observed along the range axis of MIMO ambiguity functions produced by phase codes. We propose two MIMO receiver architectures that permit to integrate mismatched filters. The first architecture tries to minimize all autocorrelations and crosscorrelations of the transmitted phase codes, while the second architecture computes mismatched filters adapted to the signals transmitted in different angular direction. The latter approach permits to obtain MIMO ambiguity function very close to the perfect thumbtack shape.**

***Index Terms*—MIMO ambiguity function, mismatched filter, quadratically constrained quadratic program.**

I. Introduction

THE detection theory states that the optimal filter for detecting a single target in gaussian noise is the matched filter that optimizes the Signal-to-Noise Ratio at the reception side [1]. Unfortunately this matched filter is optimal only in the single target case: the maximal processing gain that it provides is obtained at the cost of relatively high sidelobes that may penalize the detection in multitarget settings where weak targets are buried in the sidelobes generated by stronger targets or strong clutter. This problem arises in many applications such as classic radar range/doppler ambiguity functions, or more recently coherent MIMO radar ambiguity functions.

2-3

2 notes:

For linear chirp signals that are used in many radar applications, a possible solution to improve the sidelobe level in range is to apply weighting windows at the reception [2]. Amoung the possible weighting windows are found the famous Hamming, Hann, Kaiser, Blackman, Dolph-Chebyshev windows and many others [3]. The main drawback of this approach is a broader mainlobe and some loss in the processing gain, since the optimal matched filter has in fact been replaced by a mismatched filter.

4-5

2 notes:

For phase codes, weighting windows cannot be applied but one can find optimal filters that provide minimal Peak to Sidelobe Ratio (PSLR) [2], [4], [5]. An approach proposed first in [4] and followed in [5] to find the optimal filter consists in an Iterated Reweighted Least Square (IRLS) method based on the computation of the optimal filter providing the best Integrated Sidelobe Level (ISL), that can be easily found by solving an L_2-norm optimization problem under a linear constraint. It provides an approximate solution to the PSLR problem. A modified version of the RLS algorithm has also been proposed in [6], [7] with a minimax error criterion to reduce the PSLR. Finally a more recent approach aims at directly solving the PSLR problem by replacing the L_2-norm by an L_{2n}-norm with $n > 1$ [8]. This new optimization problem, that provides again an approximate solution to the PSLR problem, must be solved numerically. Of course, in both cases the resulting mismatched filter presents some loss in the processing gain.

The contribution of this paper is three-fold. First we propose a new approach for finding the optimal mismatched filter in the PSLR sense. The proposed approach directly solves the PSLR problem by transforming it into an equivalent Quadratic Constrained Quadratic Program (QCQP). The proposed QCQP is shown to be convex so that any feasible solution is a global solution of the problem. In that sense, our approach finds the exact solution to the PSLR problem. A rich literature exists on QCQPs, and efficient solvers have been developed based on semidefinite programming relaxation [9], [10] solved by interior point methods [11], [12]. The proposed QCQP presents also the advantage to be easily extended with additional constraints. As an instance, we show that it is possible to add constraints in order to control the loss in processing gain (LPG) of the resulting filter, the mainlobe shape or the ISL. In particular, controlling the LPG is interesting since it permits to ensure that a good PSLR is not obtained at the cost of a large LPG, or to limit the LPG to some predefined desired value. To our knowledge, such a constraint cannot easily be integrated in previous cited solutions and has therefore not been considered despite its importance. We provide some results on mismatched filters computed for Gold phase codes and chirp signals. For the phase codes, we also study on simulations the impact of phase errors or distorsions to the sidelobe level obtained with the mismatched filter. It comes that the mismatched filter is quite robust to such distorsions.

Second we propose to extend the proposed QCQP to deal with possible doppler shifts, a feature which has, to our

O. Rabaste and L. Savy are with ONERA, the French Aerospace Lab, Electromagnetic and Radar Department; BP 80100, 91123 Palaiseau, France.

knowledge, never been considered in the literature, although the mismatched filter is not very tolerant to doppler shifts. We show that additional doppler constraints are still quadratic convex and can therefore easily be inserted in the optimization program. The proposed extended QCQP permits to obtain good performance in a range of interesting radial velocities. Of course, it should still be dedicated to specific applications, for instance in digital communications, for the detection of slow-moving targets, or for the case of airborne radars. These two last cases are studied here on simulations.

The third contribution of this paper considers the specific setting of the MIMO radar. In this MIMO framework, the different transmitting antennas or subarrays transmit different signals. We consider here a MIMO system composed of colocated antennas that takes advantage of the transmitting signal orthogonality to separate the different signal contributions at the reception and retrieve the transmission phase [13], [14], [15], [16]. At the reception side, the optimal MIMO processing consists of a general matched filter in range, angles and doppler. The output of such a matched filter may be summarized through the use of the so-called MIMO ambiguity function. It has been defined and extensively studied in [17], [15], [18]. One fondamental feature of the MIMO ambiguity function is that range and angular space cannot be decoupled unless perfectly orthogonal waveforms are transmitted. Unfortunately such families of waveforms do not exist and one must face a certain amount of range/angle coupling [19]. However for phase code families such as those codes used in digital communications, for instance the Gold codes [20], the Kasami codes [21] or some chaotic codes [22], range decoupling is achieved at the cost of a spreading of the energy in the whole ambiguity domain, with relatively high sidelobe level. The use of beamforming at the reception side permits to decrease to some extent these sidelobes along the angular dimension, but high sidelobes remain along the range axis.

06 e Guinebretiere

We therefore propose here to adapt the mismatched filter strategy to improve the MIMO ambiguity function for phase codes. We remain here in the context of the detection of slow-moving targets and do not consider any doppler shifts. Two approaches are considered. First the mismatched filter is considered to improve the global orthogonality of the phase code family by improving the sidelobe levels of the autocorrelations and crosscorrelations of the codes. This approach, which is in the principle similar to the one proposed in [5] for multi-user communications, leads to a receiver architecture identical to the standard MIMO system, where the classic matched filters to each transmitted waveforms are replaced by their mismatched counterparts. The second approach consists in applying the mismatched filter on the signal received by the target instead of the different signals transmitted by the phased array antennas. Since the signal received by a target differs with the direction, several mismatched filters must be computed, one per each considered direction. This implies a certain change in the receiver architecture. This second strategy seems to provide a good solution to the sidelobe level for the MIMO ambiguity function of phase codes. Examples based on the MIMO ambiguity function computation for good chaotic codes are presented.

07 e Guinebretiere

This paper is organised as follows. In section II, we present the mismatched filter framework. The strategy proposed to find the optimal PSLR filter by solving a QCQP is developed in section III, and some simulation results are provided. In section IV, we propose an extension of the QCQP that permits to integrate doppler constraints, and we present again simulation results on two study cases. Then we turn our attention to the MIMO context. The general MIMO ambiguity function is presented in section V, as well as two strategies to adapt the mismatched filter framework to the MIMO ambiguity function. Simulation results are provided in this same section.

II. Mismatched filter

Let us consider a signal vector $\mathbf{s}$ containing N samples:

$$\mathbf{s} = [s_1, s_2, \ldots, s_N]^T.$$

In the absence of noise, the classic matched filter consists in computing the correlation vector $\mathbf{y}$ of length $2N-1$ given by:

$$\mathbf{y} = \mathbf{\Lambda}_N(\mathbf{s})\mathbf{s} \tag{1}$$

where the correlation matrix $\mathbf{\Lambda}_K(\mathbf{s})$ of size $K+N-1 \times K$ is defined by

$$\mathbf{\Lambda}_K(\mathbf{s}) = \underbrace{\begin{bmatrix} s_N & 0 & \ldots & \ldots & \ldots & \ldots & 0 \\ \vdots & s_N & \ddots & & & & \vdots \\ s_2 & & \ddots & 0 & & & \vdots \\ s_1 & s_2 & \ldots & s_N & 0 & \ldots & 0 \\ 0 & s_1 & \ddots & \vdots & s_N & \ddots & \vdots \\ \vdots & \ddots & \ddots & s_2 & & \ddots & 0 \\ 0 & \ldots & 0 & s_1 & s_2 & & s_N \\ \vdots & & & 0 & s_1 & \ddots & \vdots \\ \vdots & & & & \ddots & \ddots & s_2 \\ 0 & \ldots & \ldots & \ldots & \ldots & 0 & s_1 \end{bmatrix}}_{K \text{columns}}$$

and K represents the number of columns of $\mathbf{\Lambda}_K(\mathbf{s})$. This matched filter is known to be optimal for single target problems, i.e. it maximizes the energy at the peak response. However it does not care about the sidelobe level. Therefore it is not necessarily fit for multitarget problems, where the sidelobe level is of primary importance.

Instead of computing (1), a mismatched filter will compute the convolution between signal $\mathbf{s}$ and a different filter sequence $\mathbf{q}$ in a similar way:

$$\mathbf{y} = \mathbf{\Lambda}_K(\mathbf{s})\mathbf{q}, \tag{2}$$

where the output vector $\mathbf{y}$ is of length $K+N-1$. As we can already notice from this expression, the length K of the filter sequence $\mathbf{q}$ may be larger than the signal length N. In the following, we will assume for simplicity that $K = N+2p$ so that the length of $\mathbf{y}$ is odd, and we symetrically add the same number p of samples on both sides of the code.

Since the matched filter maximizes the Signal to Noise Ratio (SNR) at the peak response, any other filter will result in a

Loss in Processing Gain (LPG) at the peak response. This LPG can be defined as the ratio between the SNR gathered with the mismatched filter and the optimal SNR obtained with the matched filter:

$$\begin{aligned} \text{LPG} &= 10\log_{10}\left(\frac{\text{SNR}_{\text{mismatched}}}{\text{SNR}_{\text{matched}}}\right) \\ &= 10\log_{10}\left(\frac{|\mathbf{q}^H\mathbf{s}|^2}{(\mathbf{q}^H\mathbf{q})(\mathbf{s}^H\mathbf{s})}\right) \leq 0. \end{aligned} \tag{3}$$

In the literature, exact formula has been provided for computing the optimal sequence $\mathbf{q}$ that minimizes the ISL (Integrated Sidelobe Level) [4], [5]. It is obtained by solving the following optimization problem:

$$\begin{array}{rl} \min_{\mathbf{q}} & \mathbf{y}^H\mathbf{F}\mathbf{y} = \min_{\mathbf{q}} \|\mathbf{F}\mathbf{y}\|_2^2 \\ \text{s.t.} & \mathbf{s}^H\mathbf{q} = \mathbf{s}^H\mathbf{s}, \end{array} \tag{4}$$

where $\mathbf{F}$ is a diagonal matrix defined by vector $[1,\ldots,1,0,1,\ldots,1]$ with ones everywhere except for a 0 at entry $N+p$, $\|\mathbf{x}\|_n$ represents the L_n norm of vector $\mathbf{x}$, and the constraint $\mathbf{s}^H\mathbf{q} = \mathbf{s}^H\mathbf{s}$ is mainly included to discard the null solution. The analytic solution for this problem, simply obtained by using Lagrange multipliers, is

$$\mathbf{q}_{\text{ISL}} = \frac{(\mathbf{s}^H\mathbf{s})\left(\mathbf{\Lambda}_K(\mathbf{s})^H\mathbf{F}\mathbf{\Lambda}_K(\mathbf{s})\right)^{-1}\mathbf{s}}{\mathbf{s}^H\left(\mathbf{\Lambda}_K(\mathbf{s})^H\mathbf{F}\mathbf{\Lambda}_K(\mathbf{s})\right)^{-1}\mathbf{s}}. \tag{5}$$

Such a solution is optimal regarding the ISL criteria but not the PSLR (Peak to SideLobe Ratio) criteria which may be of greater interest depending on the application. Therefore an iterative algorithm based on solution (5) has been proposed to obtain an approximate solution for the PSLR problem [4], [5]. This iterative approach is very similar to Iterated Reweighted Least Squares (IRLS) methods [23]. This solution provides quite interesting results, but it relies on an heuristic and therefore leads only to an approximate solution to the PSLR problem.

Another approach has recently been considered to solve the PSLR problem. It consists in replacing the L_2 norm in the optimization problem (4) by an L_{2n} norm with n greater than 1 [8]. Analytical solution is not available anymore and numerical methods must then be considered to solve this problem. Again this approach does not provide the exact solution to the PSLR problem.

III. QCQP for mismatched filter

In this section, we propose a new approach for solving the PSLR problem. This solution consists in building a convex Quadratically Constrained Quadratic Program (QCQP) that can then be efficiently solved by numerical methods. The convexity of the proposed program insures that any found feasible solution is a global optimum of the PSLR problem [9]. Besides the flexible structure of this formulation permits to include additional constraints in the problem that may be of interest.

A. QCQP solution to the PSLR problem

Let us first define the PSLR problem. It consists in solving the following optimization problem:

$$\begin{array}{rl} \min_{\mathbf{q}} & \|\mathbf{F}\mathbf{y}\|_\infty \\ \text{s.t.} & \mathbf{s}^H\mathbf{q} = \mathbf{s}^H\mathbf{s}, \end{array} \tag{6}$$

where $\|\mathbf{x}\|_\infty = \max_i |x_i|$ represents the infinity norm of vector $\mathbf{x}$. Again the constraint is introduced in order to discard the null solution.

This problem cannot be solved analytically. However it can be equivalently cast as the following QCQP:

$$\begin{array}{rll} \min_{\mathbf{q}} & t & \\ \text{s.t.} & \mathbf{s}^H\mathbf{q} = \mathbf{s}^H\mathbf{s}, & \\ & \mathbf{q}^H\boldsymbol{\lambda}_{N+p+i}^H(\mathbf{s})\boldsymbol{\lambda}_{N+p+i}(\mathbf{s})\mathbf{q} \leq t \quad \text{for} \quad |i| \geq 1, & \end{array} \tag{7}$$

where $\boldsymbol{\lambda}_n(\mathbf{s})$ is the n^{th} row of matrix $\mathbf{\Lambda}_K(\mathbf{s})$ (to lighten the notation, we discard here the index K in the notation $\boldsymbol{\lambda}_n(\mathbf{s})$). This QCQP contains exactly $2K-1$ constraints: the first linear constraint permits to discard the trivial solution, while each of the $2(K-1)$ other quadratic constraints limits the level for each correlation sample. Note that the first constraint is linear and the other constraints are quadratic convex (since matrix $\boldsymbol{\lambda}_{N+p+i}^H(\mathbf{s})\boldsymbol{\lambda}_{N+p+i}(\mathbf{s})$ is rank 1 with positive non zero eigenvalue and is therefore positive semidefinite), while the objective is constant. Thus we have indeed defined a QCQP that is exactly identical to the PSLR problem (6) whose solution therefore exactly matches the PSLR solution.

An interesting feature of this formulation is that it permits to easily include additional constraints, as long as they remain quadratic convex. For instance it is possible to add a constraint regarding the Loss in Processing Gain (LPG) induced by the mismatched filter. Indeed, inserting in (3) the constraint of equal energies $\mathbf{s}^H\mathbf{q} = \mathbf{s}^H\mathbf{s}$, it comes that

$$\text{LPG} = 10\log_{10}\left(\frac{\mathbf{s}^H\mathbf{s}}{\mathbf{q}^H\mathbf{q}}\right).$$

Constraining the LPG to be better than some $-10\log_{10}\alpha$ dB with $\alpha \geq 1$ implies then:

$$\text{LPG} \geq 10\log_{10}\alpha \Leftrightarrow \mathbf{q}^H\mathbf{q} \leq \alpha\ \mathbf{s}^H\mathbf{s}.$$

The right hand side of the last equation is a constant, and therefore such a constraint is quadratic convex and can be inserted in the QCQP. This additional constraint is of primary importance because it permits to ensure that the good PSLR provided by the optimal filter $\mathbf{q}$ is not obtained at the cost of a large LPG, or conversely because it is possible to limit the LPG to some reasonable predefined loss.

It is also possible to add constraints on the shape of the mainlobe. Indeed in some applications it may be desired to get very low sidelobes at the cost of a larger mainlobe. It is the case for instance when using weighting windows [2]. In such a case, an easy solution consists in adding zeros in the diagonal of matrix $\mathbf{F}$ to eliminate constraints. But such a strategy does not constrain anymore the peak level in the mainlobe, that may distort the mainlobe shape. A possible remedy consists in adding fixed value constraints for the peak level in the mainlobe. More generally, it is possible to add some fixed value constraints to any samples of the filter output.

Constraining the filter output sample i to be less than a given value b_i can simply be achieved by adding the quadratic convex constraint:

$$\mathbf{q}^H \boldsymbol{\lambda}^H_{N+p+i}(\mathbf{s})\boldsymbol{\lambda}_{N+p+i}(\mathbf{s})\mathbf{q} \leq b_i$$

Finally, the general optimization problem to solve when adding LPG constraints and mainlobe constraints is the following:

$$\begin{array}{ll} \min_{\mathbf{q}} & t \\ \text{s.t.} & \mathbf{s}^H\mathbf{q} = \mathbf{s}^H\mathbf{s}, \\ & \mathbf{q}^H\boldsymbol{\lambda}^H_{N+p+i}(\mathbf{s})\boldsymbol{\lambda}_{N+p+i}(\mathbf{s})\mathbf{q} \leq t \quad \text{for} \quad |i| \geq N_{ML}, \\ & \mathbf{q}^H\mathbf{q} \leq \alpha\ \mathbf{s}^H\mathbf{s}, \\ & \mathbf{q}^H\boldsymbol{\lambda}^H_{N+p+i}(\mathbf{s})\boldsymbol{\lambda}_{N+p+i}(\mathbf{s})\mathbf{q} \leq b_i \quad \text{for} \quad |i| < N_{ML}, \end{array} \tag{8}$$

where N_{ML} is the number of samples in the right side of the mainlobe. Of course additional constraints on other correlation samples could be added if desired. Finally we can remark that a constraint on the level of ISL can also be added to the QCQP since such a constraint, that can be written as $\mathbf{q}^H\boldsymbol{\Lambda}_K(\mathbf{s})^H\mathbf{F}\boldsymbol{\Lambda}_K(\mathbf{s})\mathbf{q} \leq c_{ISL}$ where c_{ISL} is a predefined constant, is also quadratic convex. However we will not use this kind of constraint in the remainder of the article.

Note that these additional constraints may not always be inserted as simply in the L_2 of L_{2n} solutions. In particular, for the L_2 problem, these additional constraints lead to non analytical solution for the ISL problem which is the keypoint for the iterative procedure to solve the PSLR problem.

Since the proposed QCQP is convex, it can be solved very efficiently and any found solution is insured to be globally optimal. A rich literature exists for solving QCQPs, with solutions based on semidefinite programming relaxation [9], [10] solved by efficient interior point methods [11], [12]. Many softwares have been developped for solving this kind of problems. In this work, we used CVX, a MATLAB package for specifying and solving convex programs [24], [25], to solve the general convex program (8). Note that the optimization procedure is iterative and may therefore be costly, depending on the size of the problem. However in the case of mismatched filter, the computational cost is not of primary importance since the computation can be done offline.

B. Some results

In this section, we present a few results obtained with the QCQP formalism.

1) Phase code: First we study the performance obtained with a Gold sequence [20] of length $N = 127$. Figure 3.a) presents the output of the classic matched filter for such a sequence as well as the output obtained for a mismatched filter computed with the QCQP defined by equation (7) with a constrained LPG of -1 dB and a mismatched filter of the same length as the matched filter, i.e. $K = N$. The PSLR for the classic matched filter is equal to 14.5 dB while the PSLR for the mismatched filter is 23.7 dB, inducing a gain of 9.2 dB. The measured LPG for the mismatched filter reaches the constraint of -1 dB. Figure 3.b) presents the result obtained for the same sequence and $K = N$ when setting the LPG constraint to -2 dB. In that case, the PSLR for the mismatched filter is 24.6 dB, inducing a gain of 10.1 dB. Again the measured LPG reaches the objective of -2 dB. Note that for this first case, removing the constraint on the LPG provides an optimal filter with PSLR equal to 25.1 dB, i.e. a gain of 10.6 dB, at the price of an LPG of -3.7 dB. We also present in Figure 2, for completeness, a comparison between the optimal filter computed with respect to the ISL criteria and the optimal filter computed with the proposed QCQP for the PSLR optimization.

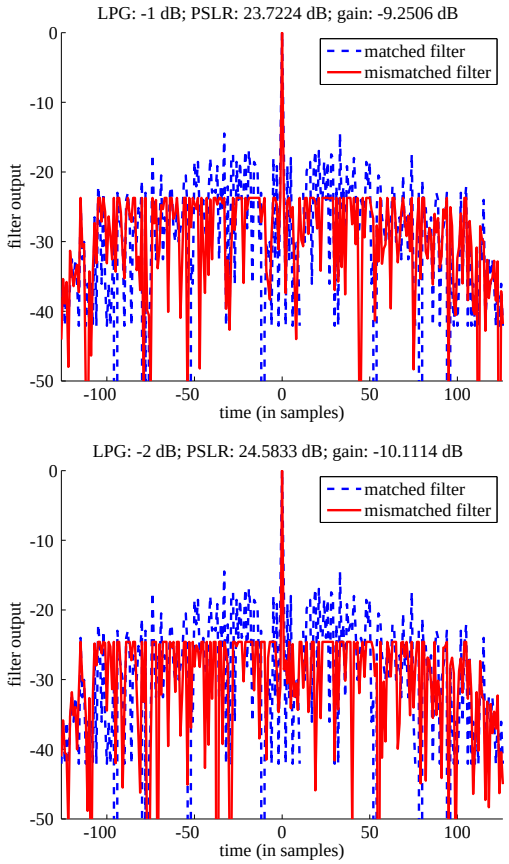

Fig. 1. Matched and mismatched filters for a Gold sequence of length $N = 127$ and a constrained LPG of: a) Top: -1 dB; b) Bottom: -2 dB. Here the length of the mismatched filter is $K = N$.

In this first setting, the length of the mismatched filter matches the length of the matched filter. It is of course possible to get improved performance by increasing the length of the mismatched filter. We present in Figure 3.a) and b) the results obtained when setting $K = 3N$. For the constraint $LPG = -1$ dB, the PSLR obtained is 26.6 dB, providing a gain of 12.1 dB, while for the constraint $LPG = -2$ dB, the PSLR obtained is 30.9 dB, providing a gain of 16.5 dB compared to the matched filter sidelobe level. For this second case, removing the constraint on the LPG provides an optimal filter with PSLR equal to 37.0 dB, i.e. a gain of 22.5 dB, at the price of an LPG of -4.7 dB.

2) Linear chirp signal: We now study the performance obtained with the QCQP formalism when applied to a linear chirp signal. The application of the mismatched filter to this type of signal was for instance considered in [8], [26]. Note that this study case is shown here only for illustration purpose:

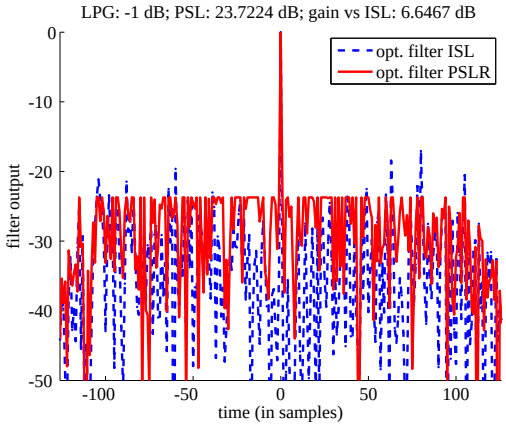

Fig. 2. Comparison of mismatched filters for ISL and for PSLR criteria for the same Gold sequence as in Figure 3.a) for an LPG of -1 dB. Here the length of the mismatched filter is $K = N$. The gain here is the difference in sidelobe level between the two mismatched filters.

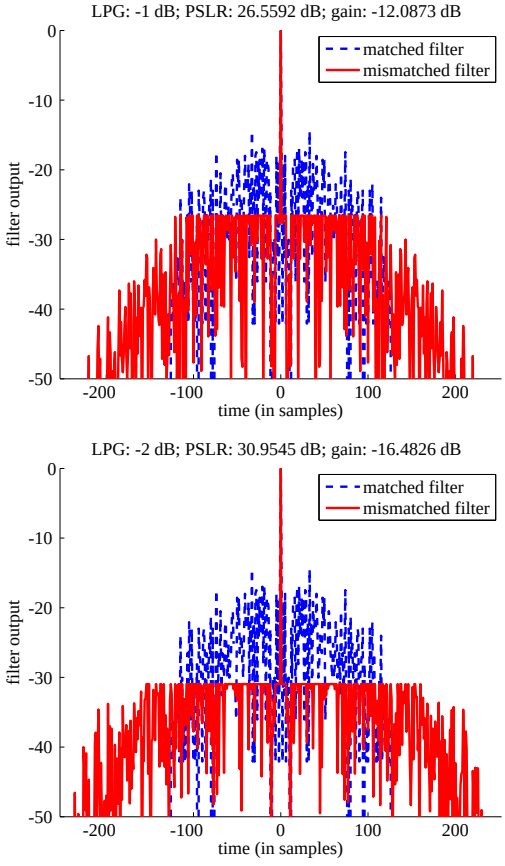

Fig. 3. Matched and mismatched filters for a Gold sequence of length $N = 127$ and a constrained LPG of: a) Top: -1 dB; b) Bottom: -2 dB. Here the length of the mismatched filter is $K = 3N$.

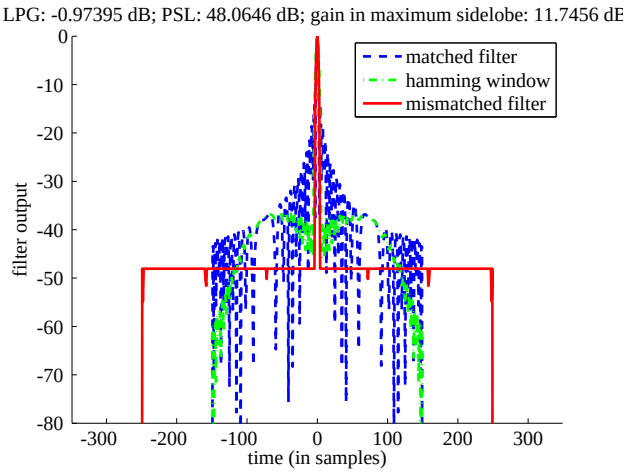

Fig. 4. Matched, hamming mismatched and optimal mismatched filters for a linear chirp signal of bandwidth $B = 2$ MHz with time-bandwidth product $BT = 50$, with a constrained LPG of -1 dB. The length of the mismatched filter is $K = 350$.

we believe that the mismatch filter is too sensitive for chirp signals with phase varying continously to be of practical interest in real applications, contrary to phase codes. We present in Figure 4 the result for a chirp signal of bandwidth $B = 2$ MHz with time-bandwidth product $BT = 50$, oversampled at a sampling frequency $f_s = 3B$, so that there are 150 samples. The length of the mismatched filter is fixed to $K = 350$, the LPG constraint is set to -1 dB and N_{ML} is set to 4, i.e. we do not put any constraint on samples included in the matched filter mainlobe. The PSLR measured is equal to 48.1 dB. For information is presented in the same figure the output when a Hamming window is used at the reception. For this Hamming window, the LPG measured is -1.4 dB. The gain obtained by the mismatched filter PSLR compared to the Hamming PSLR is equal to 11.7 dB with a mainlobe width narrower and a better LPG. Note that even better gain can be obtained by increasing the length of the mismatched filter to $K = 450$, that is exactly thrice the length of the chirp: in that case, we obtain a PSLR of 57.3 dB, i.e. a gain of 20.9 dB compare to the Hamming PSLR.

We also present in Figure 5 the result obtained when we add constraints on the mainlobe shape; here these constraints are set so that the mainlobe of the mismatched filter matches the mainlobe obtained with the Hamming window. The LPG is still constrained to -1 dB. In that case, the PSLR measured becomes 56.3 and the gain compared to the Hamming case is increased to 20.0 dB.

Remark that we provide here results for oversampled chirp signals (sampling frequency larger than B). Indeed for chirp signals, the mismatched filter should be computed for oversampled signals since the phase of the chirp varies continuously. If applied only to signals sampled at the bandwidth, larger sidelobes will appear as soon as the targets are located at non integer delays. Moreover this oversampling should be chosen large enough (at least a factor 8) in order to mitigate this phenomena. We chose here a smaller factor of 3 to speed up the computation of the mismatch filter, knowing that the

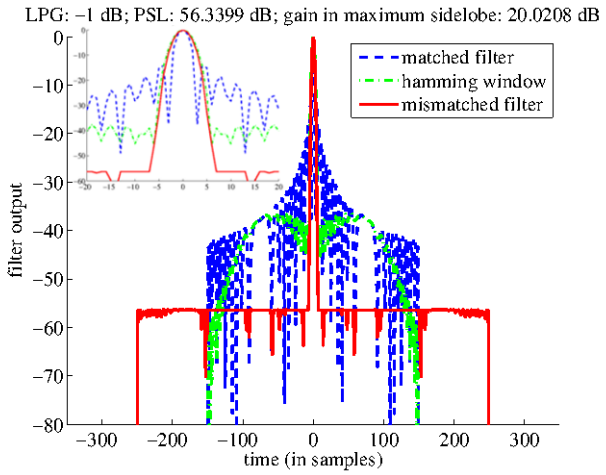

Fig. 5. Matched, hamming mismatched and optimal mismatched filters for a linear chirp signal of bandwidth $B = 2$ MHz with time-bandwidth product $BT = 50$, with a constrained LPG of -1 dB. The length of the mismatched filter is $K = 350$. The small figure inside represents a zoom on the mainlobe: the mainlobe width for the mismatched filter is similar to that obtained with the hamming window.

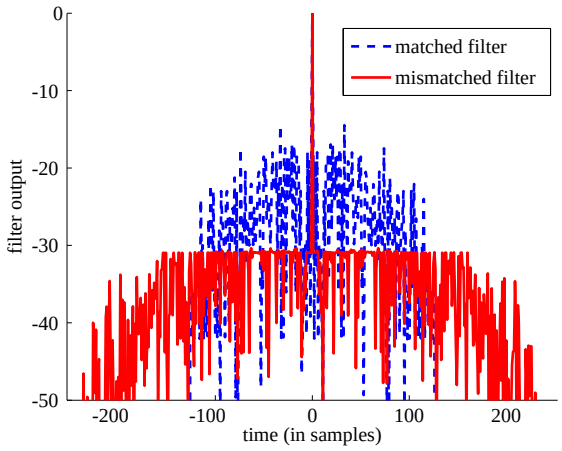

Fig. 6. Matched and mismatched filters for a Gold sequence of length $N = 127$ and a constrained LPG of -2 dB when the phase code is subject to uniform random phase errors drawn in the interval $[-5, 5]^\circ$.

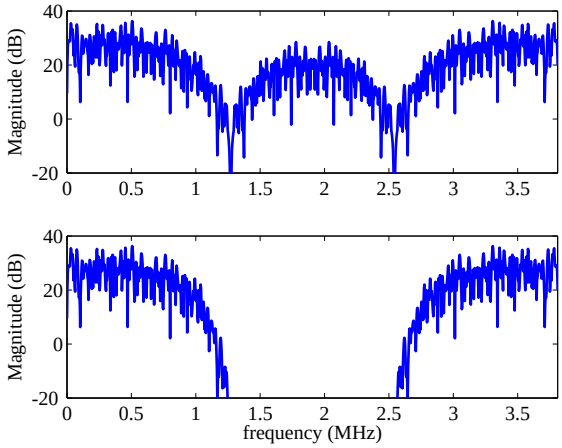

Fig. 7. Top: spectrum of a Gold sequence of $N = 127$ chips transmitted in a pulse duration $T_p = 100$ μs. Bottom: spectrum of the same sequence filtered by a low-pass filter

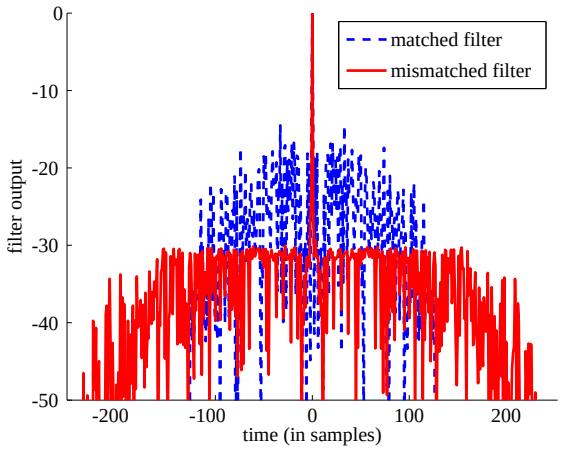

Fig. 8. Matched and mismatched filters for a Gold sequence of length $N = 127$ and a constrained LPG of -2 dB when the phase code has been filtered by a low-pass filter at the phase code bandwidth.

sidelobe level does not change much with the oversampling. Note that this problem does not arise for phase code since the phase code is constant over the chip duration so that any non integer delay will provide the same phase.

3) Robustness to phase errors: In this section we investigate the robustness of such mismatched filters to phase errors. This is important since phase errors will occur in real applications due to the imperfections of the transmitters and/or the receivers, and to some filtering steps that must be applied to the transmitted signal. We propose here to consider the robustness of the mismatched filter with respect to two kinds of errors.

First we consider random phase errors uniformly drawn in a given interval $[-\theta_{\max}, \theta_{\max}]$ where θ is the phase argument. The erroneous phase code generated can be written $\mathbf{s}_e = \mathbf{E}\mathbf{s}$ where $\mathbf{E}$ is a diagonal matrix with n^{th} element expressed as $e^{j\epsilon_n}$ where ϵ_n is a random phase error. The mismatched filter is computed on the theoretical perfect phase code and applied to the erroneous code. The result is presented in Figure 6 for $\theta_{\max} = 5^\circ$. As we can see, the mismatched filter output remains very flat. The mismatched filter can therefore be considered to be robust to such kind of errors, as long as they remain reasonable.

We consider then more realistic distorsions due to the application of a low-pass filter on the transmitted signal that cuts frequencies larger than the code bandwidth. Spectrums for the phase code and the low-pass filter output are shown in Figure 7. The mismatched filter is again computed on the theoretical perfect code and applied to the distorted code. The result is presented in Figure 8. Again the sidelobe level is very flat and we can conclude that the mismatched filter is robust to distorsions due to filtering steps. Note however that it is still better to compute the mismatched filter on the filtered signal, if the knowledge of this signal is available. This is especially true for chirp signals.

IV. Mismatched filter with doppler constraints

In the previous section, we have proposed a convex QCQP to obtain the optimal filter in the zero doppler case. Since the mismatched filter is by nature optimized for that particular doppler value, it is intrinsically not robust to doppler shifts, especially when these doppler shifts take high values. In particular, when applying the optimal filter to a doppler-shifted signal with increasing doppler values, one can observe that the maximum sidelobe level rapidly increases with the doppler-shift, reaching the level provided by the matched filter or even worse.

We propose now a modified convex QCQP that permits to take into account possible moderate doppler shifts, and therefore to mitigate this effect. Note that to our knowledge, this problem has never been considered in the literature, perhaps because the proposed solutions could not be fit easily to these additional constraints. As we will see, in the proposed framework, taking into account doppler shifts only implies to insert additional convex quadratic constraints into the convex QCQP.

A. Convex QCQP with doppler constraints

Let us denote by $\mathbf{s}^\nu$ the signal vector $\mathbf{s}$ modified by a doppler shift ν. The k^{th} component s_k^ν of $\mathbf{s}^\nu$ is provided by

$$s_k^\nu = s_k e^{j2\pi\nu k T s},$$

where T_s is the sampling period. To keep the previous notation for zero-doppler signals, we simply set $\mathbf{s}^0 = \mathbf{s}$. The output of the optimal filter $\mathbf{q}$ applied to this doppler shifted signal is given as previously by $\mathbf{y}^\nu = \mathbf{\Lambda}_N(s_k^\nu)\mathbf{q}$. Let us then consider a set of D doppler shift values $[\nu_1, \nu_2, \ldots, \nu_D]$. Finding the optimal filter $\mathbf{q}$ that minimizes both the sidelobe level for the zero doppler signal $\mathbf{s}$ and the doppler-shifted signals $\mathbf{s}^{\nu_1}, \mathbf{s}^{\nu_2}, \ldots, \mathbf{s}^{\nu_D}$ can be written as the following infinity norm minimization:

$$\begin{array}{ll} \min_{\mathbf{q}} & \| \left[\mathbf{F}\mathbf{y}^T, \left(\mathbf{F}^{\nu_1}\mathbf{y}^{\nu_1}\right)^T, \ldots, \left(\mathbf{F}^{\nu_D}\mathbf{y}^{\nu_D}\right)^T\right]^T \|_\infty \\ \text{s.t.} & \mathbf{s}^H\mathbf{q} = \mathbf{s}^H\mathbf{s}, \end{array} \quad (9)$$

where the matrix $\mathbf{F}^{\nu_d}$ is a diagonal matrix similar to the previously defined matrix $\mathbf{F}$, with the difference that it takes into account a possible shift in delay of the maximum of the output signal $\mathbf{y}^{\nu_d}$, i.e. the zero values in the diagonal will be located around entry $N + p + c(\nu_d)$, where $c(\nu_d)$ represents the number of samples corresponding to the delay shift of the maximum of the ambiguity function for the doppler shift ν_d. This is necessary for chirp signals whose ambiguity function presents a distance-doppler coupling where the maximum of the ambiguity function for a given doppler shift ν_d is located at a non zero delay. For phase codes, this will generally not be the case, i.e. $c(\nu_d) = 0$.

The presence of additional doppler outputs in the objective of problem (9) can be easily taken into account as additional convex quadratic constraints in the proposed convex QCQP, leading to the following equivalent QCQP:

$$\begin{array}{ll} \min_{\mathbf{q}} & t \\ \text{s.t.} & \mathbf{s}^H\mathbf{q} = \mathbf{s}^H\mathbf{s}, \\ & \mathbf{q}^H\mathbf{q} \leq \alpha\ \mathbf{s}^H\mathbf{s}, \\ & \mathbf{q}^H\boldsymbol{\lambda}^H_{N+p+c(\nu_d)+l}(\mathbf{s}^{\nu_d})\boldsymbol{\lambda}_{N+p+c(\nu_d)+l}(\mathbf{s}^{\nu_d})\mathbf{q} \leq t \\ & \qquad \text{for } |l| \geq N_{ML} \text{ and } d \in \{0, \ldots, D\}, \\ & \mathbf{q}^H\boldsymbol{\lambda}^H_{N+p+c(\nu_d)+l}(\mathbf{s}^{\nu_d})\boldsymbol{\lambda}_{N+p+c(\nu_d)+l}(\mathbf{s}^{\nu_d})\mathbf{q} \leq b_l^{\nu_d} \\ & \qquad \text{for } |l| < N_{ML} \text{ and } d \in \{0, \ldots, D\}. \end{array} \quad (10)$$

As we can see from this program, the constraints for signal $\mathbf{s}$ and doppler-shifted signals $\mathbf{s}^{\nu_d}$ are very similar, the only change appearing from the possible delay shift taken into account through the integer term $c(\nu_d)$. Clearly, each additional doppler value considered induces a large increase of the size of the problem since it involves a large amount of constraints $(2N + 2p - 2 - 2(N_{ML} - 1)$ constraints if no constraints on the mainlobe values are considered, $2N + 2p - 2$ constraints if constraints on the mainlobe values are used). Besides, since more constraints are considered, it is obvious that the optimal value of the PSLR will be worse at zero doppler for the optimal filter with doppler constraints that for the filter optimized only for the zero doppler.

B. Application on two study cases

We study in this section the application of the optimal filter, both as defined by QCQP (8) (no doppler consideration) and by QCQP (10) (that takes into account additional doppler constraints), on two particular applications. Note that we consider here dedicated applications, first the detection of slow-moving targets with relatively low doppler-shift using the phase code previously discussed, and second a specific case of airborne radar with very small bandwidth and pulse duration.

1) Phase code with slow-moving targets: We consider in this section the Gold code studied in the previous section, and an application to the detection of slow-moving targets. The parameters used are the same as in section III-B1. Besides we consider here that the carrier frequency is $f_c = 3$ GHz and the duration of the signal is $T_p = 100$ μs. With such parameters, the ambiguity function [2] for the Gold code at zero delay reaches its first null for a radial velocity equal to 499.6 m.s^{-1}, i.e. a target with this radial velocity cannot be detected with such a code. We will therefore consider here only targets in the range $[-500, 500]$ m.s^{-1}. Note that in the range $[0, 500]$ m.s^{-1}, the level of the ambiguity function maximum decreases continuously, but at the same time, the sidelobes provided by the optimal filter are expected to increase.

The optimal filter with doppler constraints is applied with four doppler constraints, at radial velocities equal to -450 m.s^{-1}, -250 m.s^{-1}, 250 m.s^{-1} and 450 m.s^{-1}. The matched filter, the optimal filter with no doppler constraints and the optimal filter with doppler constraints are then used to process signals with different doppler shifts in the range $[-500, 500]$ m.s^{-1}. An example of the output observed for a signal with a doppler shift of 250 m.s^{-1} is presented in figure 9. Clearly on this figure, the sidelobe level insured by the optimal filter with doppler constraints is better than the one provided by the optimal filter without these constraints. Performance is

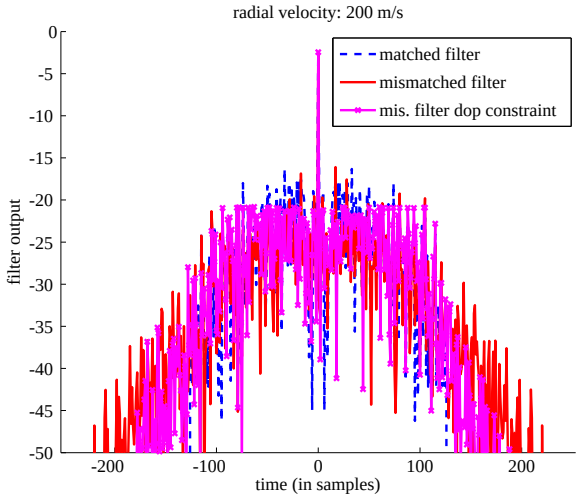

Fig. 9. Matched and mismatched filters for a Gold sequence of length $N = 127$ and a constrained LPG of -1 dB for a target with a radial velocity of 200 m.s^{-1}. Carrier frequency: $f_c = 3$ GHz; pulse duration: $T_p = 100$ μs.

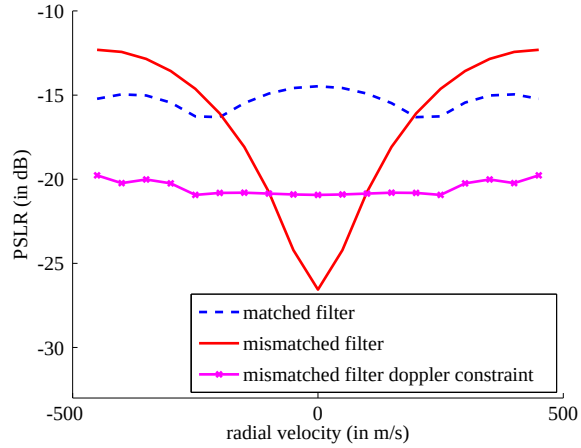

Fig. 10. PSLR with respect to radial velocity for matched and mismatched filters for a Gold sequence of length $N = 127$ and a constrained LPG of -1 dB. Carrier frequency: $f_c = 3$ GHz; pulse duration: $T_p = 100$ μs.

measured in terms of PSLR with respect to the radial velocity, and presented in figure 10. We can observe that the optimal filter with no doppler constraints is not very robust to doppler shift: its PSLR rapidly increases with the radial velocity of the target, and becomes even worse than the PSLR of the matched filter for velocities larger than 200 m.s^{-1}. On the contrary, the PSLR provided by the optimal filter with mismatched constraints remains relatively flat, and better than the matched filter in the whole velocity range.

2) Airborne radar: In airborne radar, the transmitted signal is usually a chirp with a very small time-bandwidth product, modulated by a carrier in X-band. Due to the very limited time-bandwidth product, classic windowing such as Hamming window is not fully efficient. On the contrary, due to the relatively high carrier frequency and the very short pulse duration, equivalent phase code would be relatively doppler tolerant, and thus the mismatched filter is expected to be useful in this setting.

Let us therefore consider a chirp signal of bandwidth $B = 2.66$ MHz and pulse duration $T_p = 3.75$ μs, passed first through a low-pass filter, and then transmitted with a carrier at frequency $f_c = 10$ GHz. The sampling frequency is set to $f_s = 5B$. We compute the optimal filter for this signal with a loss in processing gain constrained to -1 dB, i.e. less smaller than the LPG induced by the Hamming window (equal to -1.56 dB for that particular chirp signal), and a mainlobe width similar to that of the matched filter (i.e. narrower than the one provided by the Hamming window). Then this optimal filter is used to process signals with different doppler shifts corresponding to target radial velocities from 0 to 1200 m.s$^-1$. We compute also the optimal filter with doppler constraints. For this solution, two additional doppler constraints are used, one at $\nu = 600$ m.s^{-1} and the other at $\nu = -600$ m.s^{-1}. Note that with this specific chirp signal, the maximum of the ambiguity function for a doppler shift of $v_r = 1200$ m.s^{-1} is shifted by a delay $2v_r f_c T_p/(Bc)$ equal to 109.8 ns, that is almost one time sample since the sampling period is here $T_s = 123.5$ ns. Therefore, in this case, it is necessary to take into account this delay shift in the QCQP.

An example of the output of the two mismatched filters is presented in figure 11 for a target with a radial velocity of 600 m.s$^-1$. The tolerance to doppler shifts of the two mismatched filters is computed in terms of PSLR and compared to the matched filter and to the Hamming window. Results are presented in figure 12 with respect to the radial velocity. We can observe that the PSLR of the output of the mismatched filter is strongly dependent on the doppler shift: it becomes worse when the radial velocity of the target increases. In that sense, it is not very robust to the doppler shift. However, it should be noted that it remains better than the Hamming window for all the velocities considered, with the same LPG and a mainlobe width constrained here to the mainlobe width of the matched filter, thus narrower than the mainlobe obtained with the Hamming window (as can be observed in figure 11). As for the optimal filter with doppler constraints, it provides an almost identical level of sidelobes in the range $[-600, 600]$ m.s^{-1} that corresponds to the introduced constraints, with a level better than the matched filter and the Hamming window, but worse than the optimal filter with no doppler constraints between -500 m.s^{-1} and 500 m.s^{-1}. Outside the specified doppler range, its PSLR starts increasing but remains better than that of the optimal filter with no doppler constraints.

V. Mismatched filter for coherent MIMO ambiguity function

In this section, we will first present the coherent MIMO ambiguity function and then propose two different strategies permitting to use mismatched filters in this framework.

A. Coherent MIMO ambiguity function

Let us consider a transmitting array composed of N_E colocated antennas. In classic phased array, all antennas transmit the same waveform, and only the phase of the waveform is

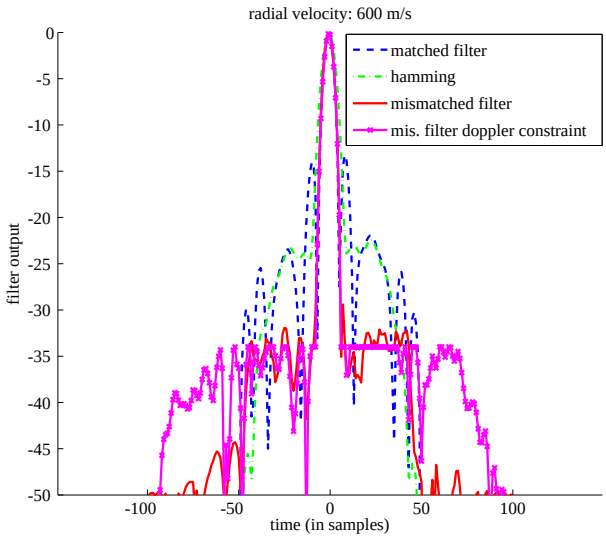

Fig. 11. Matched filter, Hamming output, and mismatched filters for a linear chirp signal of bandwidth $B = 2.66$ MHz with time-bandwidth product $BT = 10$ oversampled at a sampling frequency $fs = 5B$, with a constrained LPG of -1 dB, and a target with radial velocity of 600 m.s^{-1}. The signal has been filtered by a low-pass filter at the chirp bandwidth. The length of the mismatched filter is 150.

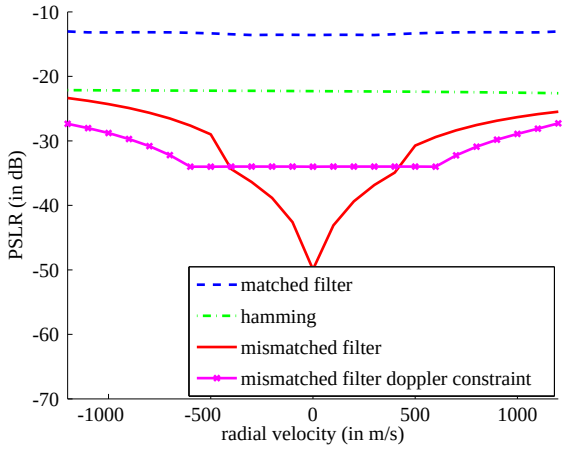

Fig. 12. PSLR with respect to radial velocity for matched filter, Hamming output, and mismatched filters for a linear chirp signal of bandwidth $B = 2.66$ MHz with time-bandwidth product $BT = 10$ oversampled at a sampling frequency $fs = 5B$, with a constrained LPG of -1 dB, and a target with radial velocity of 600 m.s^{-1}. The signal has been filtered by a low-pass filter at the chirp bandwidth. The length of the mismatched filter is 150.

different to form the beam in a given direction. In coherent colocated MIMO radar, each of the N_E antennas transmits a different waveform $s_m(t)$, so that the signal transmitted by the array in direction θ is given by

$$s(t,\theta) = \sum_{m=1}^{N_E} e^{j\mathbf{x}_{E,m}^T \mathbf{k}(\theta)} s_m(t), \tag{11}$$

where $\mathbf{x}_{E,m}$ is a vector representing the position of the m^{th} antenna, $\mathbf{k}(\theta)$ is the wave vector. Note here that in the MIMO framework, overall signals transmitted in two different

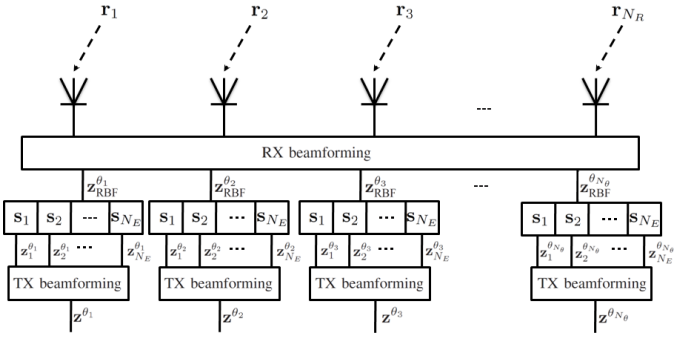

Fig. 13. Architecture at the receiver side for a MIMO radar system.

directions differ, since they result from the summation of the same codes with different phase coefficients.

Let us now assume that the reception array is composed of N_R antennas located at positions $\mathbf{x}_{R,n}$. At the reception, the optimal processing consists in computing the MIMO ambiguity function, provided by the expression [15]:

$$A(\tau,\nu,\theta,\theta_c) = \overbrace{\left(\sum_{n=1}^{N_R} e^{j\mathbf{x}_{R,n}^T(\mathbf{k}(\theta_c)-\mathbf{k}(\theta))}\right)}^{\text{Beamforming on receive}} \times \underbrace{\sum_{m'=1}^{N_E}\sum_{m=1}^{N_E} e^{j\mathbf{x}_{E,m}^T\mathbf{k}(\theta_c)-j\mathbf{x}_{E,m'}^T\mathbf{k}(\theta)}}_{\text{Beamforming on transmit}} \underbrace{\int s_m(t)s_{m'}^*(t-\tau)e^{-j2\pi\nu t}\,dt}_{\text{Cross ambiguities}}. \tag{12}$$

where τ is the delay, ν is the doppler shift, θ is the reception angle and θ_c is the true direction of the target. In this expression, we considered only one angular direction θ (azimuth or elevation) and the ambiguity function is a function of four parameters because the reception angle θ and the target angle θ_c cannot be summarized with only one angle parameter. If two angular directions were to be considered, then the ambiguity function would become a function of six parameters. The architecture for such a processing is provided in Figure 13. It consists in three steps: first, classic reception beamforming is applied to the N_R reception antenna inputs, producing N_θ outputs $\mathbf{z}_{RBF}^{\theta_j}$ corresponding to different angular directions outputs. Then to each $\mathbf{z}_{RBF}^{\theta_j}$ are applied N_E matched filters corresponding to the N_E transmitted waveforms; there are thus $N_E N_\theta$ matched filtering operations. The output of filter i applied to signal $\mathbf{z}_{RBF}^{\theta_j}$ is denoted $\mathbf{z}_{ij}$. Each input $\mathbf{z}_{RBF}^{\theta_j}$ leads to N_E outputs $(\mathbf{z}_{ij})_{i=1,\ldots,N_E}$. Finally for each direction θ_j, transmission beamforming is applied to the corresponding N_E matched filter outputs, producing one output $\mathbf{z}^{\theta_j}$ for each considered direction. Note that the order of these three steps can be changed, and reception beamforming applied only as the final stage of the processing; however such a strategy will generally lead to more computations than the one proposed here.

As can be noticed from Equation (12), the reception processing is completely decoupled in the MIMO ambiguity function, and we can therefore reduce the problem to one single reception antenna. For pulse trains, if the classic radar approximation of negligible phase rotation within the pulse stands, then the doppler effect can also be decoupled [15]. It

remains to study the following reduced ambiguity function:

$$A_r(\tau,\theta,\theta_c) = \sum_{m'=1}^{N_E}\sum_{m=1}^{N_E} e^{j\mathbf{x}_{E,m}^T\mathbf{k}(\theta_c)-j\mathbf{x}_{E,m'}^T\mathbf{k}(\theta)} \times \int s_m(t)s_{m'}^*(t+\tau)\,dt. \quad (13)$$

In this expression, no further decoupling between range and angles can be achieved unless the transmitted waveforms are perfectly orthogonal with the same autocorrelation function $\lambda_s(\tau)$ [19], i.e.

$$\int s_m(t)s_{m'}^*(t+\tau)\,dt = \lambda_s(\tau)\delta_{m,m'},$$

where $\delta_{m,m'}$ is the Kronecker operator. Unfortunately this perfect orthogonality cannot be achieved in practice although it would be desired. Some waveform families may however approach this condition [19]. Among these families, an interesting case is provided by the CDMA (Code Division Multiple Access) codes used in digital communications. These families are composed of phase codes with good autocorrelation and crosscorrelation properties. Among the well-known families used or proposed for CDMA are found the Gold codes [20], the Kasami codes [21] or more recently the chaotic codes [22]. Although Gold and Kasami codes are optimized with respect to their periodic auto and crosscorrelations, they still present acceptable aperiodic correlations. On the other hand chaotic codes are directly designed for presenting good aperiodic correlations. Besides, while Gold and Kasami families are limited to sequences of length 2^n-1, with for the Kasami family the additional limitation that n must be even, and limited also in the number of possible sequences for a given length, chaotic families are very flexible in terms of length and number of sequences, which can take any value. Therefore in the following we will consider chaotic sequences. Note that there exist many ways to generate chaotic sequences. We use here spatiotemporal chaotic sequences defined in [27] that were specifically designed for DS/CDMA systems in digital communications.

The interesting feature with such phase codes is that approximate decoupling between range and angles can be achieved, as can be seen in Figure 14 that presents the range/reception angle cut of the MIMO ambiguity function for chaotic codes of length $N = 127$ with $N_E = 4$ transmission antennas and no reception beamforming (or equivalently only $N_R = 1$ reception antenna). We observe a thumbtack type of MIMO ambiguity function. There is no noticeable coupling effect but the corresponding energy is spread over the entire parameter space with relatively high sidelobe level. This spreading comes from the summation of the non zero crosscorrelations of the different codes. It can partly be weighted by the reception processing, as can be seen in Figure 15 that present the MIMO ambiguity function of the same codes with the reception processing. However relatively high sidelobes remain along the range axis for the good angle hypothesis. There is therefore a need to decrease this level. We propose in the following sections two strategies based on the computation of mismatched filters that aim at lowering this sidelobe level.

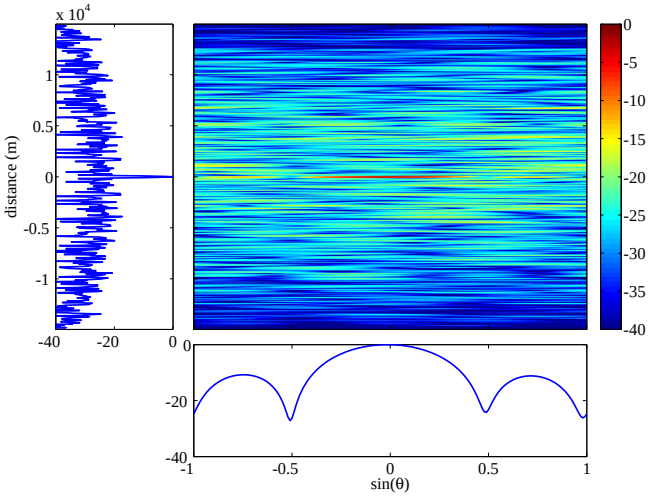

Fig. 14. Range/reception angle cut of the MIMO ambiguity function for spatiotemporal chaotic codes of length $N = 127$; $N_E = 4$ transmission antennas, no reception beamforming. Pulse duration $T_p = 100$ μs. PSLR along the range axis for $\theta = 0$: 17.3 dB.

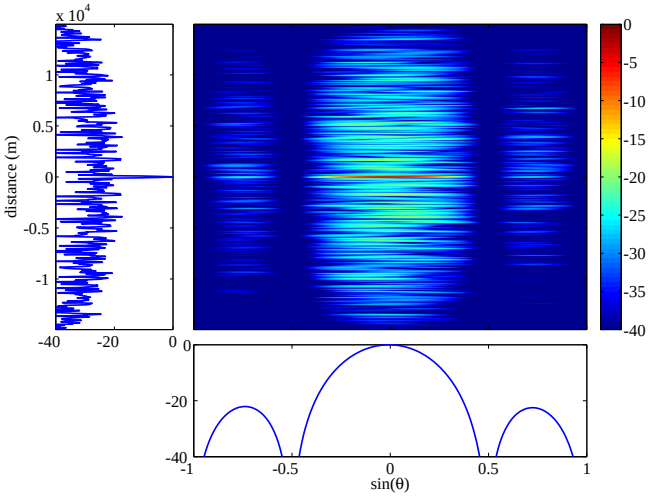

Fig. 15. Range/reception angle cut of the MIMO ambiguity function for spatiotemporal chaotic codes of length $N = 127$; $N_E = 4$ transmission antennas, $N_R = 4$ reception antennas. Pulse duration $T_p = 100$ μs. PSLR along the range axis for $\theta = 0$: 17.3 dB.

B. Mismatched MIMO receiver with transmitted sequences

The first proposed strategy consists in replacing each matched filter in architecture of Figure 13 by a mismatched filter that provides the lowest autocorrelation and crosscorrelation sidelobes; note that we use abusively here and in the following the term autocorrelation for the output of a mismatched filter corresponding to sequence $\mathbf{s}_i$ when applied to sequence $\mathbf{s}_i$ and the term crosscorrelation for the output of this mismatched filter when applied to sequence $\mathbf{s}_j$ with $j \neq i$. Let us denote by $\mathbf{s}_m = [s_{m,1}, s_{m,2}, \ldots, s_{m,N}]^T$ the phase code transmitted by antenna m, by $\mathbf{q}_m = [q_{m,1}, q_{m,2}, \ldots, q_{m,K}]^T$ the mismatched filter corresponding to code $\mathbf{s}_m$ and by $\mathbf{y}_{i,j} = \mathbf{\Lambda}(\mathbf{s}_j)\mathbf{q}_i$ the output of mismatched filter $\mathbf{q}_i$ applied to transmitted sequence $\mathbf{s}_j$. The problem of finding the optimal

filter $\mathbf{q}_i$ that minimizes both the sidelobe level of the autocorrelation output $\mathbf{y}_{i,i}$ and the sidelobe level of the crosscorrelation outputs $\mathbf{y}_{ij}$ for $j \neq i$ can be written as the following infinity norm minimization:

$$\begin{array}{ll} \min_{\mathbf{q}_i} & \| \left[\mathbf{y}_{i,1}^T, \ldots, \mathbf{y}_{i,i-1}^T, (\mathbf{F}\mathbf{y}_{i,i})^T, \mathbf{y}_{i,i+1}, \ldots, \mathbf{y}_{i,N_E} \right]^T \|_\infty \\ \text{s.t.} & \mathbf{s}_i^H \mathbf{q}_i = \mathbf{s}_i^H \mathbf{s}_i. \end{array}$$

As previously, this difficult minimization problem can be cast as the following equivalent QCQP:

$$\begin{array}{ll} \min_{\mathbf{q}_i} & t \\ \text{s.t.} & \mathbf{s}_i^H \mathbf{q}_i = \mathbf{s}_i^H \mathbf{s}_i, \\ & \mathbf{q}_i^H \boldsymbol{\lambda}_{N+p+l}^H(\mathbf{s}_i) \boldsymbol{\lambda}_{N+p+l}(\mathbf{s}_i) \mathbf{q}_i \leq t \quad \text{for } |l| \geq 1, \\ & \mathbf{q}_i^H \boldsymbol{\lambda}_{N+p+l}^H(\mathbf{s}_j) \boldsymbol{\lambda}_{N+p+l}(\mathbf{s}_j) \mathbf{q}_i \leq t \quad \text{for } |l| \geq 0 \text{ and } j \neq i, \end{array}$$

where $\boldsymbol{\lambda}_l(\mathbf{s}_j)$ is the l^{th} row of matrix $\boldsymbol{\Lambda}(\mathbf{s}_j)$. Of course it is still possible to introduce additional constraints on the LPG for filter $\mathbf{q}_i$ and on the shape of the mainlobe, thus leading to the following general optimization program:

$$\begin{array}{ll} \min_{\mathbf{q}_i} & t \\ \text{s.t.} & \mathbf{s}_i^H \mathbf{q}_i = \mathbf{s}_i^H \mathbf{s}_i, \\ & \mathbf{q}_i^H \mathbf{q}_i \leq \alpha\, \mathbf{s}_i^H \mathbf{s}_i, \\ & \mathbf{q}_i^H \boldsymbol{\lambda}_{N+p+l}^H(\mathbf{s}_i) \boldsymbol{\lambda}_{N+p+l}(\mathbf{s}_i) \mathbf{q}_i \leq t \quad \text{for } |l| \geq N_{ML}, \\ & \mathbf{q}_i^H \boldsymbol{\lambda}_{N+p+l}^H(\mathbf{s}_i) \boldsymbol{\lambda}_{N+p+l}(\mathbf{s}_i) \mathbf{q}_i \leq b_l \quad \text{for } |l| < N_{ML}, \\ & \mathbf{q}_i^H \boldsymbol{\lambda}_{N+p+l}^H(\mathbf{s}_j) \boldsymbol{\lambda}_{N+p+l}(\mathbf{s}_j) \mathbf{q}_i \leq t \quad \text{for } |l| \geq 0 \text{ and } j \neq i. \end{array}$$

Such a program is quadratic convex and can therefore be efficiently solved using CVX. Note that it contains many additional constraints compared to the single signal problem studied in section III. Thus it is not expected to provide a sidelobe level as low as one would get when solving the single signal problem.

We apply this QCQP to the chaotic sequences used for Figure 14. We first present in Figure 16 the resulting autocorrelation and crosscorrelations obtained for the mismatched filter $\mathbf{q}_1$ computed with respect to sequence $\mathbf{s}_1$, with a constrained LPG of -2 dB. Similar results are obtained for the other mismatched filters $\mathbf{q}_2$, $\mathbf{q}_3$ and $\mathbf{q}_4$. We notice that the sidelobe level is the same for the autocorrelation and the crosscorrelations; we get a PSLR equal to 21.0 dB when the PSLR for the matched filter ranges from 14.0 dB to 15.7 dB depending on the auto or crosscorrelation considered. The gain ranges between 5.3 dB and 7.0 dB, i.e. it is, as expected, much smaller than if only one sequence were considered, due to the large number of constraints (in the single sequence case, we obtain for this chaotic sequence a PSLR equal to 31.5 dB). Note that applying a constraint on the LPG is here very important. Indeed, the resulting mismatched filter with an unconstrained LPG provides a PSLR of 21.5 dB only at the price of an LPG of -5.3 dB.

We now insert the computed mismatched filters into the MIMO receiver architecture in place of the classic matched filter. The resulting MIMO ambiguity function is presented in Figure 17. The measured PSLR along the range axis for the good angle hypothesis $\theta = 0$ is equal to 20.0 dB which represent a gain of only 2.7 dB compared to the classic MIMO ambiguity function at the price of an LPG of -2 dB. Note that the PSLR for the mismatched MIMO ambiguity is larger than the PSLR obtained on the sole autocorrelation and crosscorrelations presented in Figure 16; this is because the MIMO

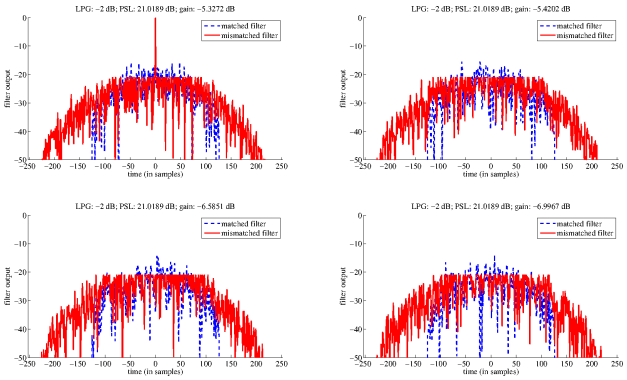

Fig. 16. Output of the mismatched filter $\mathbf{q}_1$ applied to sequences $\mathbf{s}_1$, $\mathbf{s}_2$, $\mathbf{s}_3$, and $\mathbf{s}_4$ (from left to right and top to bottom). $N = 127$ chips, $K = 3N$, LPG$= -2$ dB.

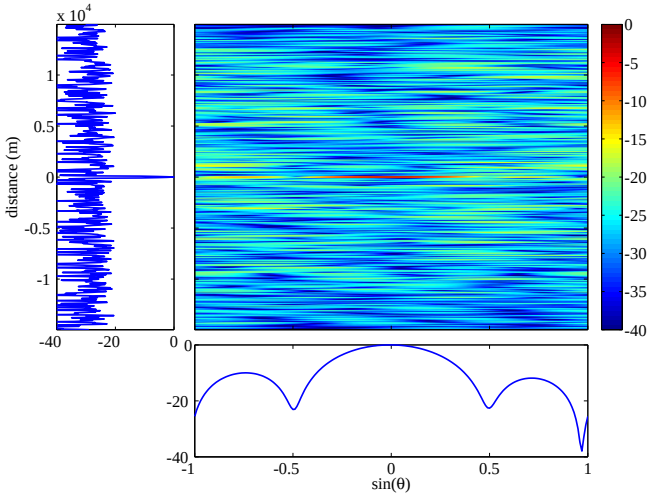

Fig. 17. Range/reception angle cut of the mismatched MIMO ambiguity function for spatiotemporal chaotic codes of length $N = 127$; $N_E = 4$ transmission antennas, no reception beamforming. Pulse duration $T_p = 100$ μs. PSLR along the range axis for $\theta = 0$: 20.0 dB.

ambiguity function mixes all auto and crosscorrelations. From this result, it appears that this first solution does not provide interesting performance.

C. Mismatched MIMO receiver with sequence received by target

As we have seen in previous section, optimizing the auto and crosscorrelation of each transmitted phase code $\mathbf{s}_i$ with respect to all other codes $\mathbf{s}_j$ for $j \neq i$ does not seem appropriate in the MIMO context. This is mainly due to the fact that the signal received by the target is a combination of all transmitted codes, so that the MIMO ambiguity function does not represent the particular output of one code with its particular autocorrelation and crosscorrelation, but rather the summation of all autocorrelations and crosscorrelations of all codes. A better strategy consists in computing directly the mismatched filter to the signal received by the target.

Let us therefore consider the signal received by a target located in direction θ_c. This signal is a linear combination

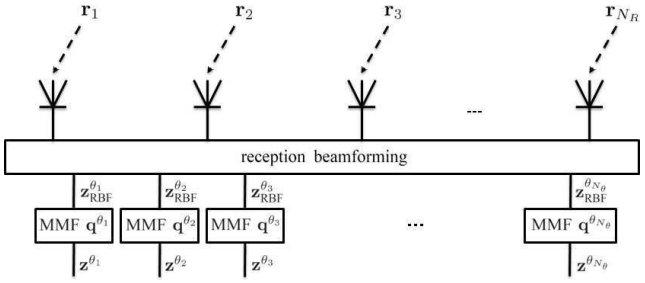

Fig. 18. Architecture at the receiver side for the proposed mismatched MIMO ambiguity function (MMF $\mathbf{q}^{\theta_i}$: Mismatched filter for direction θ_i).

of the codes transmitted by the different antennas and is given by Equation (11). It is straighforward to compute the optimal mismatched filter for this signal since it is provided by the solution of problem (8). However note that in this case the signal received by the target depends on the direction of the target. Therefore, different mismatched filters should be computed for each considered direction. This leads to a modified receiver architecture. The proposed new receiver architecture is presented in Figure 18. It consists first in applying the reception beamforming to the signals received at the different reception antennas, thus forming N_θ output signals $(\mathbf{z}_{\text{RBF}}^{\theta_i})_{i=1,\dots,N_\theta}$. Then to each considered direction θ is applied the corresponding mismatched filter $\mathbf{q}^{\theta_i}$, computed from the signal transmitted in direction θ_i. The output is then N_θ time vectors $(\mathbf{z}^{\theta_i})_{i=1,\dots,N_\theta}$, one for each considered direction. Note that in this new receiver architecture, the range matched filters and the transmission beamforming steps are somehow gathered in only one mismatched filter for a specific angle.

The result obtained with such a strategy using the same chaotic sequence as previously is presented in Figure 19. It appears that the obtained MIMO ambiguity function presents very low sidelobes along the range axis at the good angle hypothesis $\theta = 0$. The measured PSLR along that axis is equal to 35.0 dB. Further away from that range axis, the sidelobe level increases and is spread again uniformly. This result is interesting because these high sidelobes can be decreased with the reception beamforming while keeping low PSLR along the range axis. The resulting mismatched MIMO ambiguity function after reception beamforming is presented in Figure 20. We can observe that most of the sidelobes have indeed been reduced, only a fraction remaining in the mainlobe at a quite low level. This effect can even be decreased by using more antennas at the reception than at the transmission, thus reducing the reception mainlobe, as is shown in Figure 21. Finally we obtain a very clean thumbtack mismatched MIMO ambiguity function.

Note that in all these results we only presented range/reception angle cuts of the MIMO ambiguity function. However recall that there is another angular dimension represented by the true target direction. The good behavior of the mismatched filter should be checked along that direction too. We therefore present in figure 22 the range/target angle cut of the mismatched MIMO ambiguity function with the reception

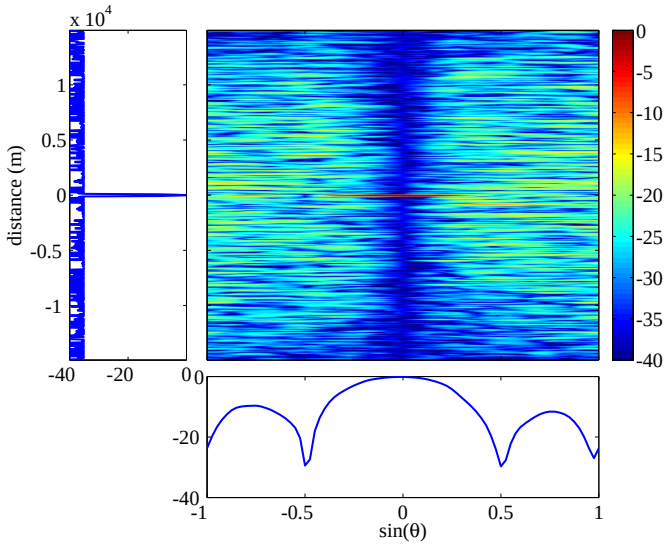

Fig. 19. Range/reception angle cut of the mismatched MIMO ambiguity function, second strategy, for spatiotemporal chaotic codes of length $N = 127$; $N_E = 4$ transmission antennas, no reception beamforming. Pulse duration $T_p = 100$ μs. PSLR along the range axis for $\theta = 0$: 35.0 dB.

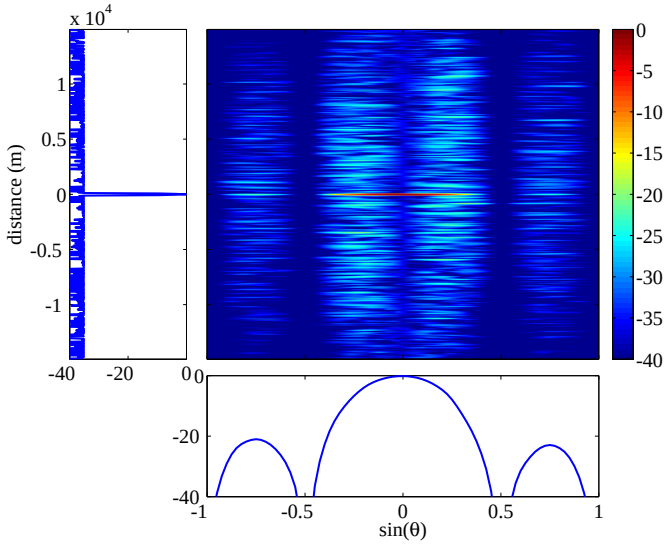

Fig. 20. Range/reception angle cut of the mismatched MIMO ambiguity function, second strategy, for spatiotemporal chaotic codes of length $N = 127$; $N_E = 4$ transmission antennas, reception beamforming with $N_R = 4$ antennas. Pulse duration $T_p = 100$ μs. PSLR along the range axis for $\theta = 0$: 35.0 dB.

beamforming. Fortunately the resulting cut is similar to the range/reception angle cut, which can be explained by the fact that the effect of the target angle is similar to the effect of the reception angle.

VI. Conclusion

In this article, we have considered the design of a filter providing the best PSLR. Contrary to methods in the literature that use heuristics to solve this problem, we define a convex quadratic constrained quadratic program equivalent to the PSLR problem that can be efficiently solved by interior point

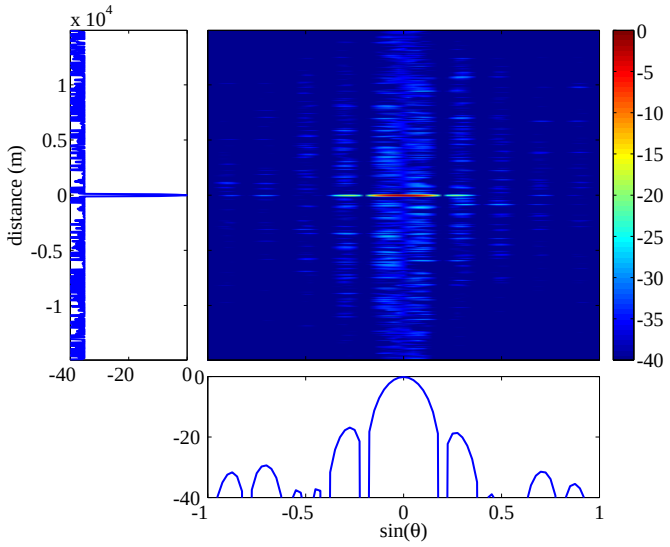

Fig. 21. Range/reception angle cut of the mismatched MIMO ambiguity function, second strategy, for spatiotemporal chaotic codes of length $N = 127$; $N_E = 4$ transmission antennas, reception beamforming with $N_R = 10$ antennas. Pulse duration $T_p = 100$ μs. PSLR along the range axis for $\theta = 0$: 35.0 dB.

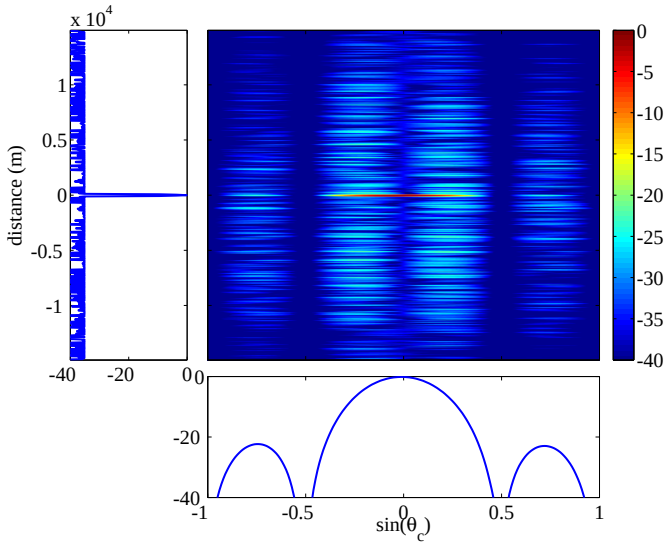

Fig. 22. Range/target angle cut of the mismatched MIMO ambiguity function, second strategy, for spatiotemporal chaotic codes of length $N = 127$; $N_E = 4$ transmission antennas, reception beamforming with $N_R = 4$ antennas. Pulse duration $T_p = 100$ μs. PSLR along the range axis for $\theta_c = 0$: 35.0 dB.

methods, and provides the optimal solution to the optimization problem. We have shown that this QCQP can be easily extended with a number of additional constraints, for instance on the loss in processing gain, the shape of the mainlobe or some doppler constraints. In particular for the doppler constraints, we have shown on simulations that, whereas the classic mismatch filter is not robust to doppler shifts, such doppler constraints can improve a lot the PSLR for non zero radial velocities. We have finally shown that such an optimal filter can be used in the MIMO radar framework. We have in particular proposed a modified processing architecture where the optimal filter is applied to the signal received by the target in different directions. This new architecture permits to improve the MIMO ambiguity function of phase codes.

It should be noted that the applications considered here are mainly radar applications, but the proposed QCQP framework for the mismatched filter is very general and could be applied to any application where a PSLR constraint is desired, for instance in digital communications, or in antenna arrays to improve the digital beamforming for nonlinear or sparse arrays. Besides many other constraints than those presented here can be added. In that sense, the proposed QCQP framework is very flexible.

REFERENCES

[1] S. Kay, *Fundamentals of Statistical Signal Processing. Detection theory*. Prentice Hall, 1998.

[2] N. Levanon and E. Mozeson, *Radar signals*. Wiley, 2004.

[3] F. Harris, "On the Use of Windows for Harmonic Analysis with the Discrete Fourier Transform," *Proceedings of the IEEE*, vol. 66, no. 1, pp. 172–204, 1978.

[4] J. Baden and M. Cohen, "Optimal peak sidelobe filters for biphase pulse compression," in *Proceedings of the IEEE International radar conference*, 1990, pp. 249–252.

[5] K. Griep, J. Ritcey, and J. Burlingame, "Poly-Phase Codes and Optimal Filters for Multiple User Ranging," *IEEE Trans. Aerospace and Electronic Systems*, vol. 31, no. 2, pp. 752–767, 1995.

[6] B. Zrnic, A. Zejak, A. Petrovic, and I. Simic, "Range sidelobe suppression for pulse compression radars utilizing modified rls algorithm," in *Proceedings of the IEEE 5th International Symposium on Spread Spectrum Techniques and Applications.*, vol. 3, 1998, pp. 1008–1011.

[7] A. Petrovic, A. Zejak, and B. Zrnic, "Ecf filter design for radar applications," in *Proceedings of the 6th IEEE International Conference on Electronics, Circuits and Systems*, vol. 2, 1999, pp. 663–666.

[8] J. Cilliers and J. Smit, "Pulse compression sidelobe reduction by minimization of Lp-norms," *IEEE Trans. on Aerospace and Electronic Systems*, vol. 43, no. 3, pp. 1238–1247, 2007.

[9] S. Boyd and L. Vandenberghe, *Convex Optimization*. Cambridge: Cambridge University Press, 2004.

[10] L. Vandenberghe and S. Boyd, "Semidefinite Programming," *SIAM Review*, vol. 38, no. 1, pp. 49–95, 1996.

[11] N. Karmarkar, "A new polynomial-time algorithm for linear programming," *Combinatorica*, vol. 4, pp. 373–395, 1984.

[12] Y. Nesterov and A. Nemirovsky, "A general approach to polynomial-time algorithms design for convex programming," Centr. Econ. and Math. Inst., USSR Acad. Sci., Moscow, USSR , Tech. Rep., 1988.

[13] J. Li and P. Stoica, "MIMO Radar - Diversity means Superiority," in *14th Annual Workshop on Adaptive Sensor Array Processing*, 2006.

[14] ——, "MIMO Radar with Colocated Antennas," *IEEE Signal Processing Magazine*, pp. 106–114, 2007.

[15] C. Chen and P. Vaidyanathan, "MIMO Radar Ambiguity Properties and Optimization Using Frequency-Hopping Waveforms," *IEEE Trans. on Signal Processing*, vol. 56, no. 12, pp. 5926–59 368, 2008.

[16] Y. Abramovich, G. Frazer, and B. Johnson, "Noncausal Adaptive Spatial Clutter Mitigation in Monostatic MIMO radar: Fundamental Limitations," *IEEE Journal of Selected Topics in Signal Processing*, vol. 4, no. 1, pp. 40–54, 2010.

[17] G. San Antonio, D. Fuhrmann, and F. Robey, "MIMO Radar Ambiguity Functions," *IEEE Journal of Selected Topics in Signal Processing*, vol. 1, no. 1, pp. 167–177, 2007.

[18] C.-Y. Chen, "Signal Processing Algorithms for MIMO Radar," Ph.D. dissertation, California Institute of Technology, 2009.

[19] O. Rabaste, L. Savy, M. Cattenoz, and J.-P. Guyvarch, "Signal Waveforms and Range/Angle Coupling in Coherent Colocated MIMO Radar," in *2013 International Conference on Radar*, 2013.

[20] R. Gold, "Optimal binary sequences for spread spectrum multiplexing," *IEEE Trans. on Information Theory*, vol. 13, no. 4, pp. 619–621, 1967.

[21] T. Kasami, "Weight Distribution Formula for Some Class of Cyclic Codes," University of Illinois, Tech. Rep. No. R-285, 1966.

[22] G. Mazzini, G. Setti, and R. Rovatti, "Chaotic complex spreading sequences for asynchronous DS-CDMA - Part I: System modeling and results," *IEEE trans. on circuits and systems*, vol. 44, no. 10, pp. 937–947, 1997.

[23] P. Green, "Iteratively reweighted least squares for maximum likelihood estimation, and some robust and resistant alternatives (with discussion)," *Journal of Royal Statistical Society*, vol. 46 sect.B, pp. 149–192, 1984.

[24] I. CVX Research, "CVX: Matlab software for disciplined convex programming, version 2.0 beta," http://cvxr.com/cvx, Sep. 2012.

[25] M. Grant and S. Boyd, "Graph implementations for nonsmooth convex programs," in *Recent Advances in Learning and Control*, ser. Lecture Notes in Control and Information Sciences, V. Blondel, S. Boyd, and H. Kimura, Eds. Springer-Verlag Limited, 2008, pp. 95–110, http://stanford.edu/ boyd/graph_dcp.html.

[26] J. Cilliers and J. Smit, "On the trade-off between mainlobe width and peak sidelobe level of mismatched pulse compression filters for linear chirp waveforms," in *Proceedings of the 6th European Radar Conference*, 2009, pp. 9–12.

[27] S. Meherzi, S. Marcos, and S. Belghith, "A family of spatiotemporal chaotic sequences outperforming gold ones in asynchronous ds-cdma systems," in *Proceedings of the 14th European Signal Processing Conference (EUSIPCO)*, 2006.

Mismatched filter optimization for radar applications using quadratically constrained quadratic programs

Rabaste, Olivier; Savy, Laurent

01 Octave Guinebretiere Page 2
17/3/2020 13:18

02 Octave Guinebretiere Page 2
17/3/2020 13:12

03 Octave Guinebretiere Page 2
17/3/2020 14:35

04 Octave Guinebretiere Page 2
17/3/2020 13:17

05 Octave Guinebretiere Page 2
17/3/2020 14:36

06 Octave Guinebretiere Page 3
17/3/2020 14:39

07 Octave Guinebretiere Page 3
17/3/2020 14:43